Available online at www.sciencedirect.com
ScienceDirect
The International Journal of Biochemistry & Cell Biology 40 (2008) 663–676
IJBCB
www.elsevier.com/locate/biocel

# Identification and characterization of a spontaneously aggregating amyloid-forming variant of human $PrP_{(90–231)}$ through phage-display screening of variants randomized between residues 101 and 112

Archana Verma [a,1], Swati Sharma [b,1], Nirmal Kumar Ganguly [a], Siddharta Majumdar [a], Purnananda Guptasarma [b], Manni Luthra-Guptasarma [a,*]

[a] *Postgraduate Institute of Medical Education and Research (PGIMER), Chandigarh 160012, India*
[b] *Institute of Microbial Technology, Sector 39-A, Chandigarh 160036, India*

Received 7 June 2007; received in revised form 3 September 2007; accepted 5 October 2007
Available online 13 October 2007

**Abstract**

The N-terminal 'unstructured' region of the human prion protein [$PrP_{(90–231)}$] is believed to play a role in its aggregation because mutations in this region are associated with seeding-independent deposition disorders like Gerstmann–Straussler–Scheinker disease (GSS). One way of examining the effects of such mutations is to search combinatorially derived libraries for sequence variants showing a propensity to aggregate and/or the ability to interact with prion molecules folded into a β-sheet-based conformation (i.e., β-PrP or $PrP^{Sc}$). We created a library of $1.8 \times 10^7$ variants randomized between positions 101 and 112, displayed it on filamentous bacteriophage, and 'spiked' it with a ∼25% population of phages-bearing wild-type prion (wt-PrP). Screening was performed through four rounds of biopanning and amplification against immobilized β-PrP, and yielded three β-PrP-binding populations: wt-PrP (26% representation) and two non-wt-PrP variants (∼10% and ∼64% representation, respectively). The remarkable enrichment of one non-wt-PrP variant (MutPrP) incorporating residues KPSKPKTNMKHM in place of KGVLTWFSPLWQ, despite its initial representation at a 5 million-fold lower level than wt-PrP, caused us to produce it and discover: (i) that it readily aggregates into thioflavin-T-binding amyloids between pH 6.0 and 9.0, (ii) that it adopts a soluble β-sheet based monomeric structure at pH 10.0, (iii) that it is less thermally stable and more compact than wt-PrP, and (iv) that it displays significantly greater resistance to proteolysis than wt-PrP. Our results suggest that sequence variations in the 101–112 region can indeed predispose the prion for aggregation.


*Keywords:* Prion aggregation; Protein misfolding; Phage display; Sequence variants; Amyloid formation; Conformational transition

## 1. Introduction

In its normal form, the prion protein, $PrP^c$, is a GPI-anchored, metal-binding, cell-surface polypeptide folded into a predominantly α-helical conformation (Prusiner et al., 1982). In its abnormal or diseased form, the same polypeptide chain adopts a predominantly β-sheet conformation, $PrP^{Sc}$, which engages in intermolecular interactions to deposit into fibrillar amyloid aggregates. The switching of conformation from $PrP^c$ to $PrP^{Sc}$ is widely believed to occur through a contact-based molecular mechanism in which infective $PrP^{Sc}$ aggregates function as templates directing the structural remodeling of $PrP^c$ through direct molecule–molecule

* Corresponding author. Tel.: +91 172 2755196; fax: +91 172 2744401/5078.
*E-mail address:* mguptasarma@yahoo.com (M. Luthra-Guptasarma).
[1] These authors contributed equally to the work.

1357-2725/$ – see front matter 
doi:10.1016/j.biocel.2007.10.009

interactions, causing $PrP^{c}$ to be cast in the image of $PrP^{Sc}$. This conversion is believed to be responsible for the increase in deposited quantities of $PrP^{Sc}$ in the diseased state. $PrP^{Sc}$ differs from $PrP^{c}$ in its physico-chemical properties. It is insoluble even in mild detergents in contrast to $PrP^{c}$ which is soluble. Furthermore, $PrP^{c}$ is sensitive to degradation by proteases, whereas limited proteolysis of $PrP^{Sc}$ by proteinase K results in N-terminally truncated fragments with a molecular mass of 27–30 kDa, designated as PrP 27–30 (Safar et al., 2005).

In certain naturally occurring, genetically derived mutants of the prion polypeptide, the conformational switch from $PrP^{c}$ to $PrP^{Sc}$ is believed to occur spontaneously, obviating the need for exogenous 'infection' by $PrP^{Sc}$ particles. In two well-known diseases, Gerstmann–Straussler–Scheinker (GSS) syndrome and Creutzfeldt–Jacob disease (CJD), mutations are linked directly to the spontaneous appearance and amplification of the $PrP^{Sc}$ conformation (Collinge, 1997; Prusiner, Scott, De Armond, & Cohen, 1998). Certain naturally occurring mutations in the human population associated with these diseases locate in a region in the N-terminal section of the prion protein between residues 101 and 112 (Goldfarb et al., 1992; Huang et al., 1994; Leclerc et al., 2001; Riek et al., 1996). It has been proposed that semi-structured hinges, or loops bridging substructures within the prion could be destabilized by mutations occurring in this region, making the prion more prone to undergoing spontaneous misfolding into the $PrP^{Sc}$ conformation. Notably, the entire region between residues 90 and 112 is thought to be loosely structured and lacks defined secondary structure, even though it appears to play an important role in the switching of conformations between the α-helical and β-sheet states (James et al., 1997); in particular, residues 101, 108, and 111–113, have been shown to participate in structurally stabilizing hydrophobic interactions with the C-terminal sections of the protein (Barron et al., 2001; Levy, Hanan, Solomon, & Becker, 2001; Supattapone et al., 2001). It is possible, therefore, that naturally occurring mutations in this region destabilize key interactions of the region with other regions and cause it to dissociate away from the C-terminal of the prion molecule in the $PrP^{c}$ conformation, thereby increasing the scope for its structural remodeling through contact with $PrP^{Sc}$. According to available NMR spectroscopic data, recombinant prion protein contains a well-structured C-terminal region consisting of three α-helices and two very short β-strands, whereas the N-terminal region of the molecule is highly flexible (Zahn et al., 2000). If perchance the helical structure of the C-terminal region were to happen to be dependent, at least kinetically, on packing interactions with residues from the flexible N-terminal region, it would be conceivable for mutations in the N-terminal region to facilitate the profound molecule-wide helix-to-sheet conversion accompanying amyloid formation. Thus, regions such as the stretch between residues 101 and 112 which contain naturally occurring mutations predisposing individuals to prion disease become worthy of further attention.

In order to understand the molecular events underlying the conversion of $PrP^{c}$ to $PrP^{Sc}$, studies have relied on heterologous expression systems in order to obtain sufficient quantities of protein for biophysical studies. For most studies, the region of the reading frame spanning residues 90–231 of human PrP (corresponding to PrP 27–30) has been cloned and expressed in *E. coli*. This segment encompasses the entire sequence of the protease-resistant protein found in prion diseased brain, and contains all known point mutations associated with human prion disorders, and is sufficient for the propagation of the disease (Leffers et al., 2004).

To further explore the importance of this region, we used the phage-display library-based screening approach, developed over a decade ago as a rapid selection method for identification of protein variants with altered binding characteristics to a known ligand (Smith & Scott, 1993). As is widely acknowledged, this approach allows one to simultaneously make qualitative and semi-quantitative analyses of the binding properties of a large number of variants within a single 'competition' experiment, to select the best binding variants. Given the difficulties of obtaining and working with $PrP^{Sc}$, we decided to use as the ligand a β-sheet-based unimolecular form of the prion protein called β-PrP which is generated through the refolding of prion protein under reducing conditions at acidic pH (Jackson et al., 1999b). We immobilized β-PrP and allowed it to interact with a phage-displayed library of prions varying in respect of their sequences between residue positions 101 and 112.

We hoped, specifically, to examine (i) whether the region between residues 101 and 112 is important for the conformational switching mechanism, by examining whether sequence changes in this region facilitate, under physiological conditions, the adoption of a β-sheet conformation by prion molecules displayed on phage. Without the attendant complications of aggregation, the adoption of the β-sheet-based conformation could imaginably occur through induction involving association with β-PrP bound to a solid substrate. Alternatively, it could also occur through the natural adoption of a β-sheet-based conformation incidentally capable of binding to β-PrP, i.e., capable of interaction with immo-

bilized β-PrP, allowing phage-display library screening and identification as a β-PrP-binding variant. In other words, adoption of the β-sheet structure by a variant prion could constitute the cause, rather than the consequence, of interactions with β-PrP. We also hoped to examine (ii) whether the prion polypeptide in the $PrP^c$ conformation (i.e., wt-PrP, as a control) itself also displays a tendency to switch conformation from an α-helical form to a β-sheet-based form and bind to β-PrP, in competition with a large number of mutant, potentially structurally destabilized forms capable of undergoing the same structural transition.

A phage library of mutant proteins can be produced through either the individual randomization of key residue positions, one at a time, or through the simultaneous collective randomization of all positions assumed to be important. The latter approach can offer a much more exhaustive scope for panning of the available 'sequence space' (i.e., sampling of $20^n$ variations instead of the $20 \times n$ variations sampled by the former approach; where $n$ indicates the number of positions being varied); in particular, where variations at many neighboring locations appear to be important and one is seeking a 'proof-of-principle' demonstration of the importance of a stretch of sequence, rather than the discovery of very specific single-site mutations.

Therefore, we opted to completely randomize a 12 residue region lying in the N-terminus of the prion polypeptide $PrP_{(90–231)}$ (residues 101–112) by varying all 12 positions simultaneously, and screening for binding to β-PrP. We report here the isolation of two variants. One of these variants is shown to be spontaneously amyloid forming. We also report that wt-PrP (an α-helical molecule) appears to bind to β-PrP, a unimolecular β-sheet-based form of the prion, presumably by switching into a β-sheet-based conformation itself. Interestingly, however, wt-PrP appears to show a six orders of magnitude lower tendency to bind to β-PrP than the two variants, suggesting that the latter may be some sort of 'super-prions', that straightaway deposit into amyloid fibers instead of simply possessing an apparent predisposition to do so.

## 2. Methods

### 2.1. Cloning, expression, purification and refolding of wt-PrP to α and β forms

The intron-less gene segment encoding $PrP_{(90–231)}$ was amplified from genomic DNA isolated from human blood using the oligonucleotide, ATG CGG TAC CGC TAG CGG ATC CGG TCA AGG AGG TGG CAC CCA CAG T, as the forward primer, F1 (incorporating BamHI and NheI sites) and the oligonucleotide, TTC AAG CTT ACG CGT TAA GCT TGC TCG ATC CTC TCT GGT AAT AGG C, as the reverse primer, R1 (incorporating HindIII and MluI sites). Using standard protocols, the PCR product was digested with BamHI and HindIII, and ligated into the polylinker site of the pQE-30 vector (Qiagen) to encode $PrP_{(90–231)}$ in genetic fusion with an N-terminal 6XHis histidine-affinity tag. Following transformation into *E. coli* JM109, and subcloning into SG13009[pREP4] using amp/kan screening, the integrity of the construct was confirmed through sequencing on an ABI Prism310 sequencer. SG13009[pREP4] cells induced to express $PrP_{(90–231)}$ were lysed in 8 M urea and the protein purified through standard procedures using Ni-NTA agarose (Qiagen). Refolding under oxidizing conditions was done by the method of Jackson et al. (1999a). The refolded product obtained was examined by far-UV circular dichroism (CD) spectroscopy, and electrophoretic evaluation of susceptibility to proteinase K digestion, for assessment of whether it was analogous to $PrP^c$, i.e., the α-helical form of the prion protein (α-PrP). Separately, purified protein was also refolded into the predominantly β-sheet-containing form, β-PrP, under acidic and reducing conditions by the method of Jackson et al. (1999a) at pH 4.0, and checked for conversion to the β-PrP using CD spectroscopy and proteinase K digestion after transfer to pH 8.0. The β-sheet conformation is known to be stable for upto a week after transfer to pH 8.0 (Jackson et al., 1999b). CD measurements were carried out with α-PrP and β-PrP concentrations of 0.2 and 0.46 mg/ml, respectively.

### 2.2. Construction of a phage-display library of PrP variants

Incorporation of randomization in residues 101–112 of $PrP_{(90–231)}$ was carried out through two steps. Briefly, (i) custom-synthesis was used to create a degenerate set of oligonucleotides incorporating a randomized sequence of 36 bases (corresponding to the 12 residues), flanked by 23 bases on either side corresponding to regions naturally flanking the residues. Using these oligos as forward primer, F2 [GTG GCA CCC ACA GTC AGT GGA $AC(NNS)_{12}$ GCT GGT GCT GCA GCA GCT GGG GC; where N is A, C, G, or T (equimolar) and S is G or C (equimolar)], R1 as reverse primer, and the DNA encoding $PrP_{(90–231)}$ as template (300 ng), the library of F2 primers was incorporated into a construct extending upto the 3′ end of the DNA encoding $PrP_{(90–231)}$. Further, (ii) this library (438 bp; 600 ng) was

used as template in a reaction in which F1 and R1 were used as forward and reverse primers for splicing by overlap extension (SOE), using the 14 base overlap of F1 with the template. It may be noted that the product of Step (i) was used as template in Step (ii) without gel purification, so that some DNA encoding the original wt-PrP prion would also exist in the library, for reasons detailed in discussion relating to our need to spike the library with wt-PrP-bearing phages. The spliced product (470 bp) from Step (ii) was gel purified, digested with NheI and MluI (500 units of each enzyme per 25 μg of vector), repurified (yield ≈7.6 μg) and cloned into the phage-display vector, fdtetTA74 (Sampath, Abrol, & Chaudhary, 1997), obtained as a gift from Dr. V.K. Chaudhary (Dept. of Biochem., Univ. of Delhi) through 25 separate ligation reactions using a molar ratio of 1:6 for vector: insert, with 1 μg vector in each reaction, and 3 units of T4 DNA ligase in volumes of 10 μl each, in 4 °C overnight ligations. The ligation products were pooled, ethanol-precipitated and electro-transformed into competent JM109 *E. coli* cells that secreted the encoded phages. Amplification of the library of secreted phages was done by growing transformed cells in media containing tetracycline at 37 °C for 12 h, followed by harvesting of phage by PEG/NaCl treatment. Centrifugation at 12,000 × *g* for 20 min resulted in precipitation of phage comprising the library of PrP variants. Phage titers were estimated in terms of plaque-forming units (pfu)/ml by standard methods (Smith & Scott, 1993).

### 2.3. Screening of the library of variants for binding to β-PrP

For coating of 6XHis-tagged β-PrP, His-Sorb (Qiagen) strips were used. The protein (β-PrP) which had been created through refolding in pH 4.0 buffer under reducing conditions was transferred to pH 7.5 buffer immediately before coating. There were three reasons for doing the coating at pH 7.5: (i) the 6XHis tag on the β-PrP could be expected to bind to Ni-NTA only at basic pH (at acidic pH, the nitrogen on the imidazole ring becomes protonated causing the histidine residues in the tag to lose affinity for Ni-NTA); (ii) it is known (Jackson et al., 1999a) that β-PrP retains its β-sheet conformation for several days in pH 7–8 buffer following transfer from buffer of pH 4.0, i.e., the β-sheet dominated unimolecular conformation shows sufficient kinetic stability to be subjected to coating and phage-display biopanning; (iii) it was desirable to perform biopanning with the library of $PrP_{(90–231)}$ variants at a pH close to physiological pH, so that any spontaneous aggregation shown by a prion variant could be considered to be biologically relevant and feasible. Thus, immediately following transfer from pH 4.0 buffer, approximately 50 μg of β-PrP in 200 μl of pH 7.5 buffer (10 mM Tris containing 10 mM sodium acetate) were subjected to overnight incubation in one well of a 96-well microtiter plate, with a control sample (lacking prion, but including blocking agents) incubated similarly in a different well. Following overnight incubation with β-PrP, and requisite washing procedures, equivalent amounts of input library phage were incubated in both wells to effect biopanning, following which phages were eluted, titered and amplified using standard procedures (Parmley & Smith, 1988; Smith & Scott, 1993). Four such cycles of biopanning and amplification were carried out; in each cycle the input phage used from the previous round of amplification was carefully ensured to be $2 \times 10^{11}$. Following each cycle, the eluted phage was titered through plating of an aliquot mixed with host strain XL1-Blue onto LB/tet/X-gal/IPTG plates and counting of plaques. About 20 plaques were picked up for PCR amplification using $PrP_{(90–231)}$ specific primers (as detailed earlier) and sequenced on an ABI Prism 310 sequencer.

### 2.4. Creation of the recombinant mutant (MutPrP) selected through phage display

Fig. S5 of the supplemental data shows the scheme of creation of MutPrP. We first introduced mutations in the region spanning the residues 101–112 using a custom-synthesized primer (Mut Primer). This primer had an overlap (with the wild-type PrP gene) of 26 bases on the 5′ end and 17 bases on the 3′ end of the region incorporating the mutations [shown in red color in Fig. S5]. The first PCR step was carried out using the Mut Primer as forward primer and Primer 2 as reverse primer. This PCR product was shorter than the DNA segment needed to encode the full length $PrP_{(90–231)}$, and so another PCR reaction was carried out using Primer 1 as forward primer and Primer 2 as reverse primer to synthesize the gene for full length MutPrP (spanning residues 90–231 along with appropriate 5′ and 3′ extensions for subsequent restriction digestion and ligation into the vector). The sequences of the primers are mentioned below:

*Primer 1* (*forward primer*): **5′** ATG CGG TAC CGC TAG CGG ATC CGG TCA AGG AGG TGG CAC CCA CAG T **3′**.
*Primer 2* (*reverse primer*): **5′** TTC AAG CTT ACG CGT TAA GCT TGC TCG ATC CTC TCT GGT AAT AGG C **3′**.
*Mut Primer* (*forward primer*): **5′** GTG GCA CCC ACA GTC AGT GGA ACA AGG GCG TCC TCA CGT

GGT TCA GCC CGC TCT GGC AGG CTG GTG CTG CAG CAG C **3′**.

The final PCR product was double digested with BamHI and HindIII restriction enzymes and finally cloned into these very sites in the pQE 30vector.

### 2.5. Protein concentration estimations

Absorbance of protein solutions was measured at 280 nm ($A_{280\,nm}$) using a Cary 50 UV–Visible spectrophotometer. The absorbance was converted to protein concentration on the basis of the theoretically predicted absorption coefficients calculated by Vector NTI software. For wt-PrP, an $A_{280\,nm}$ of 1.0 was taken to correspond to a concentration of 0.89 mg/ml. For MutPrP, an $A_{280\,nm}$ of 1.0 was taken to correspond to a concentration of 0.57 mg/ml. The drop in the concentration of MutPrP for an absorbance of 1.0 was due to the introduction of two tryptophan residues in the altered sequence between residues 101 and 112. It may be noted that estimation of protein concentrations based on predicted absorption coefficients is the next-best method of determining protein concentrations to the use of actual known absorption coefficients determined through the primary measurement of the amounts of non-hydrolysable amino acids generated upon acid hydrolysis of peptide bonds. Especially for proteins differing profoundly in aromatic amino acid content, this method is preferable to measurements based on other indirect colorimetric methods that tend to be skewed by differential aromatic contents.

### 2.6. Gel filtration chromatography

The gel filtration elution behavior of wt-PrP and MutPrP was studied on a Pharmacia SMART system. Pumps and columns were washed with filtered Millipore Elix-3 water and pre-equilibrated with buffers of appropriate pH corresponding to the sample pH. The column used was the micro-analytical Superdex-75 (Amersham Biosciences; bed volume ∼2.4 ml). The volume of sample loaded was 50 μl. Samples were loaded onto the column for either purification or in analytical mode. The elution volumes were compared with the elution profiles of the standards run on the same column.

### 2.7. Fluorescence spectroscopy

Fluorescence spectroscopy was carried out on a Perkin-Elmer spectrofluorimeter (LS-50B) or on a Jasco J810 spectropolarimeter fitted with an emission monochromator. Tryptophan fluorescence spectra: For fluorescence emission spectra of proteins, the excitation wavelength was set at 280 or 275 nm and the emission spectrum recorded between 300 and 400 nm. The excitation/emission band passes used were either 5/5, 10/10 or 5/10 nm. Scan speeds were set at 100 or 120 nm/min and all spectra were averaged over 5 or 10 scans. Thioflavin T (ThT) fluorescence spectra: thioflavin T is a reagent known to become strongly fluorescent upon binding to amyloid fibrils through intercalation into the cross-β-structure formed by polypeptide chains in these fibrils. ThT-binding studies for detection of amyloids were performed by incubating protein solutions or microsuspensions in 6 μM solution of thioflavin T (in 10 mM Tris, pH 8.0) for 1 hr and recording the emission spectrum (455–550 nm) using an excitation wavelength of 444 nm. Excitation and emission slits were set at 7 nm and scan speed was set at 100 nm/min. Control spectra were collected for buffer containing ThT but no protein, as well as for buffer containing ThT and another protein (lysozyme, 0.2 mg/ml).

### 2.8. Circular dichroism spectroscopy

Far-UV CD spectra were collected for wt-PrP and MutPrP in buffers of pH 10.0, or pH 8.0 as necessary on a Jasco J-810 CD spectropolarimeter in cuvettes of 1.0 cm/0.5 cm/0.2 cm path length, with flushing of Iolar grade I nitrogen gas at 6–12 l/min. The wavelength range of data collection was mostly 250–190, or 250–200 nm. Data integration time used was approximately 1 s/nm. The raw ellipticity obtained was converted to mean residue ellipticity $[\theta]$ in deg cm$^2$ dmol$^{-1}$, using the formula: $[\theta] = \{\theta_{obs}$ in millidegrees $\times$ 100 $\times$ MRW$\}/\{1000 \times$ protein concentration (in mg/ml) $\times$ path length (in cm)$\}$, where MRW (mean residue weight) was equal to the total molecular weight of the protein/total number of amino acids. For CD data at a single wavelength, e.g. in thermal melt scans, heating was carried out using the Peltier accessory of the J-810 instrument at 3 °C/min for both wt-PrP and MutPrPm using a buffer of pH 8.0 for the former, and pH 10.0 for the latter.

### 2.9. FTIR spectroscopy

FTIR spectra were collected using a Spectrum BX spectrometer (Perkin-Elmer) between 4000 and 600 cm$^{-1}$ using a resolution of 1 cm$^{-1}$ and by averaging 32 scans. The solid aggregated sample of MutPrP was resuspended in water, deposited on the inner surface of one $CaF_2$ window of a double window demountable FTIR cell, and allowed to dry completely before the cell

was assembled and subjected to scanning. The region of interest in the spectrum is between 1700 and 1600 $cm^{-1}$, where the amide I absorption band for peptide bonds is characteristic of the secondary structural content of the protein.

### 2.10. Electron microscopy

Transmission electron microscopy (TEM) of the protein aggregates was done on a JEOL 1200 EX2 instrument using the standard procedure of negative staining with phosphotungstic acid (PTA) and uranyl acetate.

### 2.11. MALDI-TOF mass spectrometry

MALDI-TOF mass spectrometry was performed on an Applied Biosystems Voyager DE-STR instrument. Protein samples were prepared by mixing with equal volume of the matrix, Sinapinic acid. Approximately 1 μl of protein sample was added to 1 μl of the matrix and spotted and dried on sample plates. Samples were set up in duplicates or triplicates. The matrix stock solutions (10 mg/ml) were prepared in 0.3% TFA (trifluoroacetic acid) and 50% acetonitrile.

### 2.12. N-terminal sequencing

Sequencing of the 14 kDa band was done in the following manner. The contents of the entire gel were transferred through electro-blotting onto a PVDF membrane (immobilon $P^{SQ}$, Sigma Chemical Co.), using the electro-transfer accessory of a BioRad Mini-Protean II apparatus. The blot was stained by the dye amido black [0.1% amido black (Sigma Chemical Co.) in 1% acetic acid]. The band on the stained PVDF blot was excised from the dried membrane, cut into small pieces and destained with 50% methanol. Then it was thoroughly rinsed with water and allowed to dry. This was then loaded onto the ABI 476A protein sequencer (Applied Biosystems).

## 3. Results

### 3.1. Cloning, expression, purification and folding of $PrP_{(90–231)}$ into α-PrP and β-PrP

As described in the Experimental section, the segment of the intron-lacking gene encoding the prion protein between residues 90 and 231 [$PrP_{(90–231)}$] was amplified from human genomic DNA and cloned into the vector pQE-30 (Qiagen) to produce a fusion at the N-terminus with a 6XHis affinity tag (Fig. S1A). The tag was added to facilitate ease of purification using Ni-NTA (nickel-nitrilotriacetic acid) conjugated sepharose resin-based affinity chromatography, and also for facile immobilization of $PrP_{(90–231)}$ on Ni-NTA coated His-Sorb plates (Qiagen) after conversion into a β-sheet-based conformation, for screening for binding to populations of phage-displayed variants.

Expression levels of the fusion protein amounted to roughly 20% of cellular protein (Fig. 1A), with the protein present mainly in the form of intracellular inclusion bodies. Pure wt-PrP polypeptide (18.2 kDa) was obtained through affinity chromatography under reducing, denaturing conditions. The polypeptide chain was then oxidized and refolded into α-PrP at pH 8.0 to produce native $PrP_{(90–231)}$, as confirmed by circular dichroism spectroscopy (Fig. S2) and by its susceptibility to proteinase K digestion (Fig. S3A). Separately, the $PrP_{(90–231)}$ polypeptide was also refolded into the β-sheet-based conformation (β-PrP) at pH 4.0, under reducing rather than oxidizing conditions, and far-UV CD spectra (Fig. S2) and proteinase K digestion (Fig. S3B) were used to confirm the formation of the relatively more protease-resistant β-sheet-based structure under these conditions.

### 3.2. Creation and characterization of the library of prion variants

A schematic of the strategy used to construct the library of $PrP_{(90–231)}$ variants randomized between 101 and 112 is shown in Fig. 2. Data relating to the intermediate stages of construction of the library (PCR1 and PCR2), together with evidence of incorporation into the phage-display vector fdtetTA74 is shown in Fig. S1B and C. The transformation of the phage vector occurred at an efficiency of approximately $1 \times 10^6$ clones/μg of DNA. Through sequencing of clones picked at random, it was discovered that roughly three-fourths of the clones contained unique sequences differing from the native sequence in the region between residues 101 and 112, whereas one-fourth sequences contained DNA identical to that of the original gene [wt-$PrP_{(90–231)}$]. This wt-PrP component of the library originated from the amplification of a small amount of the gene encoding $PrP_{(90–231)}$ left over as a template in the reaction tube from the first PCR reaction (Step I; see Fig. 2) used to create the library; thus allowing the library to contain phages-bearing wt-$PrP_{(90–231)}$. Cells transformed with phage were grown in media containing tetracycline to amplify the phage. A total of 25 μg of DNA was transformed. Given the efficiency of transformation and the observed fraction of unique sequences

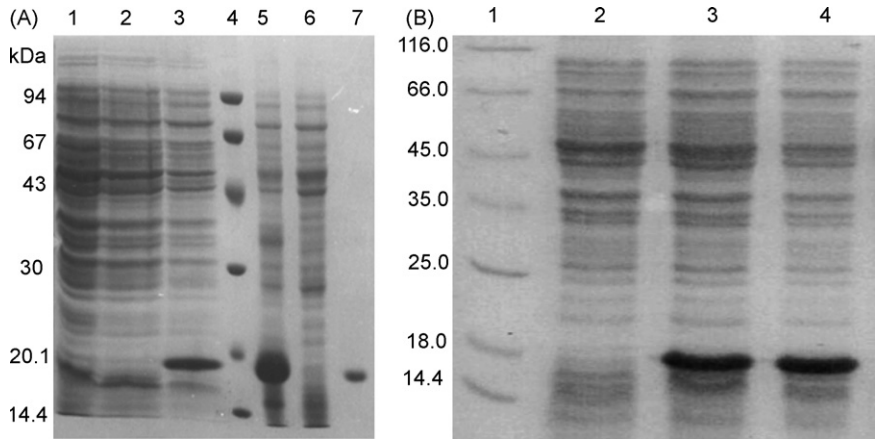


Fig. 1. Panel A: Coomassie stained 15% SDS-PAGE of various steps in the purification of human $PrP_{(90–231)}$. Total cell extract obtained upon IPTG induction of cells carrying pQE-30 without (PrP) insert (lane 1); total cell extract of cells carrying pQE-30 with PrP without induction (lane 2); total cell extract of cells carrying pQE-30 with PrP upon induction with IPTG (lane 3); molecular weight markers, as indicated on the left of the image (lane 4); insoluble protein fraction obtained as pellet, after solubilization with 6 M GdnCl (lane 5); flow-through from the Ni-NTA column of the sample loaded in lane 5 (lane 6); pooled fractions obtained after elution of protein bound to Ni-NTA column, upon elution with 50 mM imidazole solution (lane 7). Panel B: Expression of the recombinant MutPrP in *E. coli* SG13009 cells. Lane 1: Molecular weight markers; lanes 2–4: cell lysates showing MutPrP expression at 0 h (just before induction), at 2 and 4 h after induction, respectively.

among transformants, the library's diversity was estimated to be of the order of about $1.8 \times 10^7$. Perusal of the sequences and occurrence-frequencies of nucleotides as a function of their positions in the codon (supplemental data Table 1) is instructive, in that the negligible representation of A and T residues at the third position reveals that the synthesis of the degenerate region of the oligo occurred as desired. It may be noted that whereas equimolar occurrences of nucleotides introduced during synthesis is anticipated for the first and second codon positions, the deviations in frequencies observed could reflect aspects of biological selection. Harvesting of phage from the entire culture yielded approximately $4.5 \times 10^{12}$ pfu/ml.

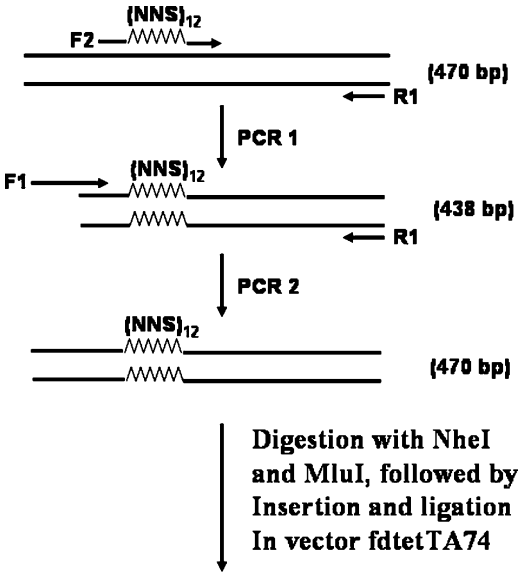


Fig. 2. Two-step construction of prion variants randomized in the region between residues 101 and 112 in $PrP_{(90–231)}$. The human PrP gene (Fig. 1) was used as a template for the PCR reaction in the first step (PCR I), with primers F2 (incorporating the degenerate sequence used for randomization), and R1, producing gene fragments containing the randomized $[(NNS)_{12}]$ residues. In the second step (PCR II), primers F1 and R1 were used, followed by digestion with NheI and MluI and subsequent ligation into the phage-display vector.

### 3.3. Screening of the library of prion variants

The library of prion variants displayed on the surface of bacteriophage was screened for ability to bind to immobilized β-PrP through four rounds of biopanning and amplification to identify variants capable of adopting, by inference, a β-sheet-based conformation in unimolecular fashion (i.e., as molecules displayed on the surfaces of single phages which interact with β-

Table 1
Nucleotide distribution in the variable region of infectious phage randomly selected from the library

| | Frequency of each base by position in codon (%) | | |
|---|---|---|---|
| Base | 1 | 2 | 3 |
| G | 32 | 34 | 54 |
| A | 16 | 13 | 3 |
| T | 31 | 25 | 4 |
| C | 17 | 24 | 35 |

Table 2
Titer of phage (in pfu/ml) obtained after each of the four rounds of biopanning and amplification

| Number of biopanning cycles | Titer of unamplified eluate (pfu/ml) | Titer of amplified eluate (pfu/ml) |
|---|---|---|
| 1st cycle | $1.5 \times 10^6$ | $1 \times 10^{13}$ |
| 2nd cycle | $3.3 \times 10^{10}$ | $4.1 \times 10^{12}$ |
| 3rd cycle | $1.9 \times 10^{10}$ | $2.3 \times 10^{13}$ |
| 4th cycle | $1.3 \times 10^{10}$ | |

PrP). Table 2 lists the titer of phage eluted and amplified after each round of biopanning. The input phage in each round was $2 \times 10^{11}$. In the control well, in the absence of β-PrP, with the same amount of input phage used, biopanning resulted in no elution of phages, confirming that there was no non-specific binding of phage particles with the His-Sorb plates [pre-blocked to prevent binding of any substance lacking Ni-NTA-binding function]. Note, however, that while the recombinant prion was produced in fusion with the His-tag to facilitate purification, conversion to β-PrP, and immobilization on the His-Sorb plates, the prion displayed was not produced in fusion with a His-tag; this was to ensure that phage do not bind to the His-Sorb plates at any stage of the screening, even by chance, as an additional precaution over and above the blocking done prior to screening. As seen from Table 1, phage eluted in the first round was amplified roughly $10^7$-fold and because the number of input phages in each cycle was the same, in the second round of biopanning there was effectively a much stronger competition among β-PrP binding-competent phages, each of which was now present in sufficient numbers to saturate, if possible, all binding sites individually. This competition was made progressively more intense through successive rounds of biopanning and amplification, each round amplifying the titers of the best binding variants. After the completion of the fourth round of biopanning several of the plaques were individually picked up for sequencing.

### 3.4. Details of β-PrP-binding variants identified selected through screening

The translated sequences of the residues in the region between 101 and 112 found to be encoded by 19 plaques picked randomly, and their frequency of occurrence, were as follows: (i) KGVLTWFSPLWQ (12 out of 19 sequences); (ii) VRLLDLTSGVSM (2 out of 19 sequences); (iii) KPSKPKTNMKHM (5 out of 19 sequences). The last sequence which occurred 5 out of 19 times was identical to wt-PrP, indicating that $PrP^c$ (in the form of wt-PrP) can also bind to β-PrP, although clearly much more poorly because no significant change occurs in the fraction population of wt-PrP recovered through four rounds of biopanning and amplification; in contrast, the other two sequences would appear to have climbed up through a nearly 5 million-fold representational handicap with respect to wt-PrP, to ultimately rival, or exceed, the numbers of wt-PrP present after the fourth round. We decided to produce and purify the first variant constituting 12 out of 19 sequences, or 64% of the sequenced population, which contained residues 'KGVLTWFSPLWQ' between positions 101 and 112 instead of the residues 'KPSKPKTNMKHM'. This variant is given the name MutPrP.

### 3.5. Characterization of wt-PrP and MutPrP produced for biophysical studies

Vector-NTI (Invitrogen) based bioinformatic analyses of wt-PrP and MutPrP (sequences shown in Fig. 3) predict their molecular masses to be 17.7 and 17.8 kDa respectively. The predicted isoelectric points (p*I*s) of the two proteins, however, differ significantly; the p*I* of wt-PrP is predicted to be 8.0, while that of MutPrP is 9.06. The aromatic residue contents and absorption coefficients of the two proteins too are predicted to be quite different. An absorbance of 1.0 at 280 nm corresponds to a protein concentration of 0.89 mg/ml for wt-PrP and 0.57 mg/ml for MutPrP. The mass of the wt-PrP produced in *E. coli* (seen in Fig. 1A) was determined to be 17.7 kDa by MALDI-TOF mass spectral analysis (Fig. S4A). We investigated the proteolytic susceptibility of this recombinant protein through a controlled proteolysis reaction with subtilisin, a non-specific protease known to cut any exposed peptide bond (using a 1:300 molar ratio of the protease to the soluble purified wt-PrP). Interestingly, subtilisin cleavage yielded a 14 kDa species along

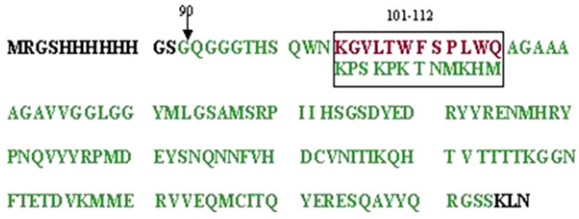


Fig. 3. The entire sequence of the recombinant $PrP_{(90–231)}$ produced in *E. coli*. The wild-type prion (wt-PrP) 90–231 sequence is shown in green with the sequence corresponding to 101–112 of the mutant shown in red. The residues from the vector are represented in black. (For interpretation of the references to color in this figure legend, the reader is referred to the web version of the article.)

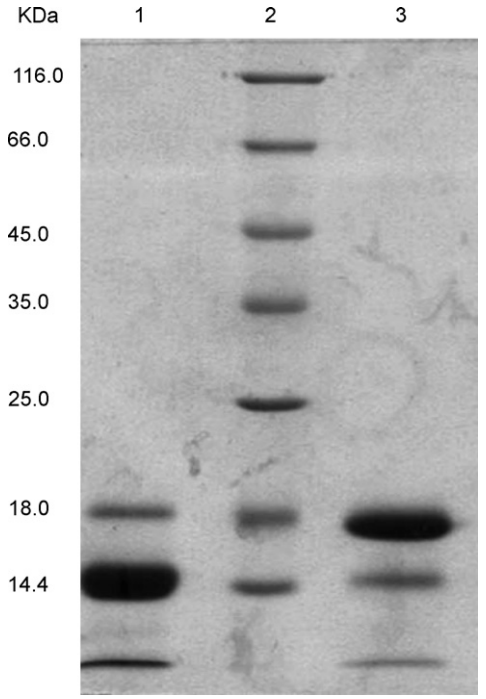


Fig. 4. SDS-PAGE showing the state of wt-PrP and MutPrP samples one week after removal of denaturant following purification, in the absence of protease inhibitors. Lane 1: wt-PrP; lane 2: molecular weight markers; lane 3: MutPrP.

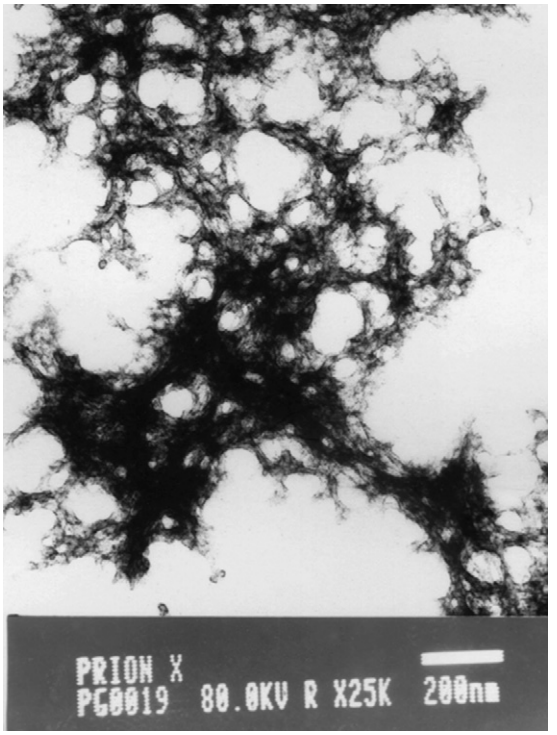


Fig. 5. Transmission electron micrographs of MutPrP deposited into a meshwork of amyloid filaments.

with a smaller peptide fragment (data not shown); the same cleavage, generating the same 14 kDa species was also seen to occur naturally in wt-PrP upon storage for a week, or more, in the absence of protease inhibitors (lane 1; Fig. 4), ostensibly through trace amounts of proteases present naturally. N-terminal sequencing was done for this 14 kDa species after elution from SDS-PAGE, and this showed that the scission generating this fragment occurs just outside the 101–112 sequence, beginning with the sequence 'GAAAAGAV' at residue 114.

Recombinant MutPrP (cloned as per the schematic shown in Fig. S5; cloning data shown in Fig. S6A) showed good overexpression in *E. coli* cells (Fig. 1B). It was purified by Ni-NTA affinity purification chromatography under denaturing conditions (Fig. S6B) and its the mass too was confirmed by MALDI TOF analysis (Fig. S4B) and found to be 17.9 kDa.

### *3.6. MutPrP is soluble at pH 10.0 but aggregates into amyloids at pH 6.0–9.0*

Whereas wt-PrP was very soluble at pH 8.0, MutPrP showed a marked tendency to precipitate at this pH, and indeed over the range of pH spanning 6.0–8.0 and above. Examination of MutPrP aggregates by TEM, revealed that they had a fibrillar morphology rather than an amorphous morphology (Fig. 5), consisting of mostly meshworks of fibrils. We also collected an FTIR spectrum of the aggregates (Fig. S7) which revealed a broad absorption band characterized by similar absorption intensities at 1625 and 1655 $cm^{-1}$, indicative of a secondary structure dominated by β-sheet content, with some content of random coil and α-helical structures. As is well known, in the FTIR spectrum of the α-helical prion protein, the absorption intensity at 1655 $cm^{-1}$ is more than twice that at 1625 $cm^{-1}$ on account of the high α-helical content (Zhang et al., 1995). Further, to examine whether the material deposited into fibrils was truly of an amyloid nature, we evaluated it for thioflavin T (ThT) binding and fluorescence. The emission spectrum of resuspended MutPrP microaggregates in the presence of 6 μM ThT (in 10 mM Tris, pH 8.0) shows a marked emission maximum at ∼482 nm (Fig. 6A) indicating that the aggregated material binds ThT and is, therefore, of 'amyloid' nature. The corresponding controls for buffer containing ThT and buffer containing ThT in the presence of 0.2 mg/ml lysozyme (showing no ThT fluorescence) are shown in Fig. S8. Since MutPrP deposited into amyloid aggregates at pH 8.0 (as well as over the

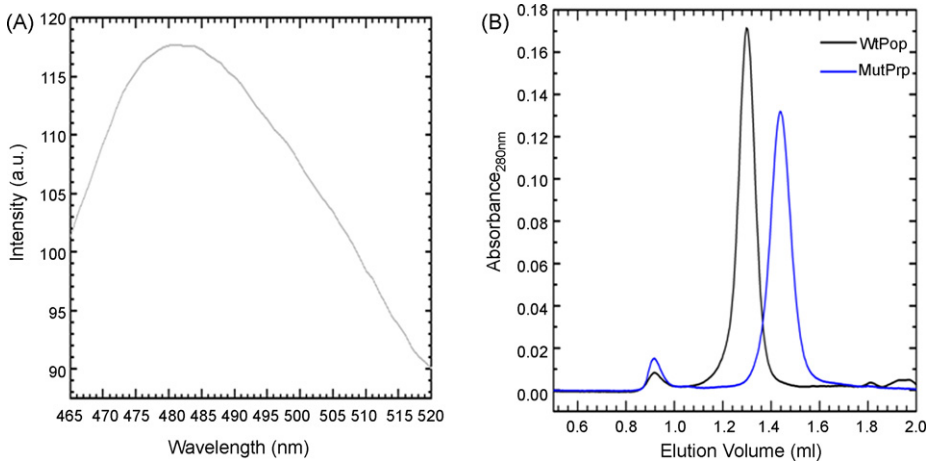


Fig. 6. Panel A: Emission spectrum of MutPrP aggregates in the presence of 6 μM thioflavin T, with excitation performed at 444 nm. Panel B: Gel filtration elution profiles of wt-PrP (in black) and MutPrP (in blue) on a Pharmacia Superdex-75 column. (For interpretation of the references to color in this figure legend, the reader is referred to the web version of the article.)

entire pH range of 6.0–9.0; data not shown), we examined its solubility at pH 10.0 and discovered that it is soluble.

### 3.7. Soluble MutPrP is monomeric like wt-PrP

Since wt-PrP was also soluble at pH 10.0, we carried out a comparison of the elutions of wt-PrP and MutPrP on a Superdex-75 SMART gel filtration column in 0.1 M carbonate buffer of pH 10.5 (Fig. 6B). Both proteins elute as single, homogenous populations. However, wt-PrP elutes at 1.3 ml and MutPrP elutes somewhat later at 1.43 ml. The elution of wt-PrP at 1.3 ml corresponds to the expected elution volume for a 17.7 kDa monomeric protein, whereas the elution of MutPrP at 1.43 ml indicates that it either (a) adopts a somewhat more compact structure than wt-PrP, with a smaller hydrodynamic volume, or (b) that the MutPrP molecule has more exposed hydrophobicity than wt-PrP which causes it to interact with the column matrix and elute at a later volume than expected, since Superdex resins are known to interact nominally with proteins exposing hydrophobic surfaces.

### 3.8. The N-terminus of soluble MutPrP is more buried

Fluorescence emission scans of the wt-PrP and MutPrP were also done under the same buffer conditions, at pH 10.0, to examine the emission status of the tryptophan residues of the two molecules following excitation with ultraviolet light of 280 nm. The sole tryptophan residue of wt-PrP at residue position 99 appears to be exposed to the aqueous solvent, giving rise to emission at ∼352 nm (Fig. 7). This observation agrees with previous studies which suggest that the N-terminal region of the wt-PrP protein containing residues 90–231 tends to be loosely structured. We also see a shoulder in the region of ∼305 nm for wt-PrP that owes either to the weaker emission of tyrosine residues or to Raman scattering from the solvent due to the 280 nm excitation. In contrast, the data with MutPrP is very interesting (Fig. 7). MutPrP has two additional tryptophan residues at positions 106 and 111, in addition to the one at position 99. Since all three residues are in what is widely thought to be a loosely structured region, MutPrP too would ordinarily be expected to emit maximally at ∼352–353 nm. Instead, the emission maximum is seen to locate at 348–349 nm, suggesting that MutPrP's tryptophans are somewhat buried through conformational alteration, and

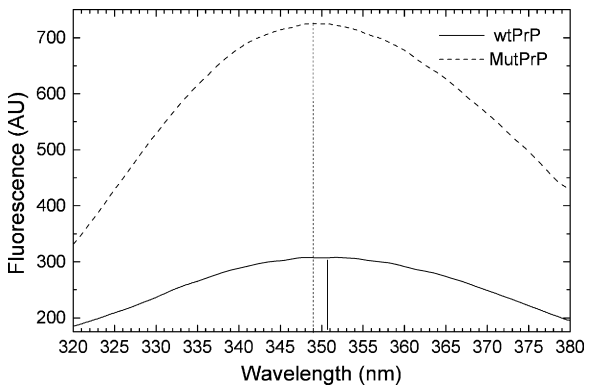


Fig. 7. Fluorescence emission spectra of wt-PrP and MutPrP upon excitation with 280 nm light.

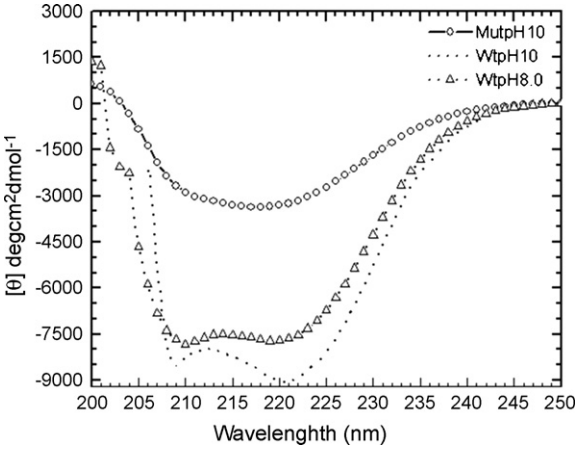


Fig. 8. Far-UV CD spectra of wt-PrP at pH 8.0 and 10.0, and MutPrP at pH 10.0.

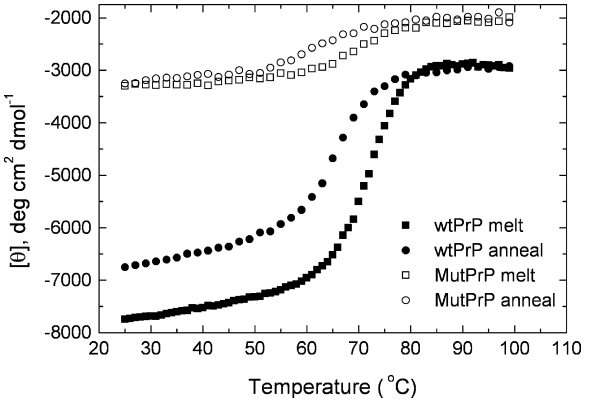


Fig. 9. Thermal melting behavior of wt-PrP at pH 8.0 and MutPrP at pH 10.0 assessed by monitoring of changes in the protein sample's mean residue ellipticity at 220 nm as a function of increasing and decreasing temperature between 25 and 99 °C.

that the region containing residues 106 and 111 is not as unstructured in MutPrP as in wt-PrP.

### *3.9. At pH 10.0, soluble MutPrP has β-structure whereas wt-PrP has α-structure*

We next evaluated secondary structure formation in wt-PrP and MutPrP at pH 10.0 by CD spectroscopy in the far-UV region. It is observed that wt-PrP adopts a typically α-helical structure under these conditions (i.e., it is helical at pH 10, just as it is already known to be helical at pH 8.0) as evidenced by the characteristic negative bands at 222 and 208 nm (Fig. 8A). In contrast, at pH 10.0, MutPrP adopts a structure with a secondary structural content and a CD spectrum typical of the β-sheet structure with a negative band at 216–218 nm, and a considerably lower overall negative ellipticity (Fig. 8B). Remarkably, the characteristics of this CD spectrum are similar to those of wild-type PrP in β-conformation (β-PrP) as reported earlier by others (Jackson et al., 1999a) and also observed by us (Fig. S2). The important difference to note is that this spectrum is seen for a variant of wt-PrP (MutPrP) at pH 10.0 which was obtained without using any reducing agent, whereas β-PrP was obtained under reducing, acidic conditions.

Thus, MutPrP naturally adopts a β-sheet conformation at pH 10.0. We might also conclude that MutPrP adopts a β-sheet conformation at pH 8.0, and indeed over the entire range of pH values at which it shows aggregation, because amyloids (which are formed) are known to be made up of β-sheets, and the cross-β-sheet structure in amyloids binds thioflavin T and causes it to show a characteristic fluorescence, which was seen with MutPrP.

### *3.10. Soluble MutPrP is of marginally lower thermostability than wt-PrP*

We next evaluated the thermal melting behavior of wt-PrP and MutPrP. Although we had measured the CD spectrum of both proteins earlier at pH 10.0, for comparison, for this experiment we took wt-PrP at pH 8.0 and not at pH 10.0, because wt-PrP is most stable at this pH, but compared its thermal stability to that of MutPrP at pH 10.0. During heating of the two proteins from 25 to 99 °C at a rate of 5 °C/min, their changes in mean residue ellipticity at 220 nm were plotted as a function of change in temperature. MutPrP starts to melt earlier than wt-PrP, at around 60 °C, whereas structure melting in wt-PrP starts around 65 °C (Fig. 9), and shows a different midpoint of the thermal melting transition ($T_m$). Also, in the case of wt-PrP, the structure is not completely regained upon reversing the temperature (cooling back to 25 °C) but in the case of MutPrP, we see almost a complete reversal upon cooling.

## 4. Discussion and conclusions

NMR solution studies have suggested that the N-terminal region of the human prion protein is flexible and loosely structured whereas the C-terminal region (mainly spanning residues 125–224 of the prion polypeptide chain) is well structured into α-helices (Zahn et al., 2000). Interestingly, however, the N-terminal region between the residues 90–112, despite its lacking defined structure, appears to play an important role in the conformational switching (James et al., 1997; Peretz et al., 1997). Residues in this region have

been shown to participate in key structurally stabilizing hydrophobic interactions with the C-terminal sections of the protein (Barron et al., 2001; Levy et al., 2001; Supattapone et al., 2001). Also, as already mentioned, in numerous instances it has been observed that mutations leading to disease locate in this N-terminal region and it may be that semi-structured hinges, or loops, bridging substructures within the prion could be destabilized by such mutations, making the prion more prone to spontaneous misfolding to the $PrP^{Sc}$ conformation (Goldfarb et al., 1992; Huang et al., 1994; Leclerc et al., 2001; Riek et al., 1996). It has been suggested that a structural conversion from the α-helical structure to the β-sheet rich form might involve a monomeric species rich in β-sheet structure. One group (Jackson et al., 1999b) has shown that in acidic reducing conditions, it is possible to cause $PrP^{c}$ to switch from its α-helical conformation to a compact, highly soluble, monomeric form rich in β-structure (β-PrP).

Given the above background, we decided to examine the importance of the N-terminal region of the prion protein (indicated by the location of naturally occurring mutations in the region and also by structural–biochemical studies), through the route of phage-display library creation and screening of sequence variants covering the region 101–112 for binding to β-PrP. To increase competition for β-PrP binding between variants and to check whether wt-PrP prion also binds to β-PrP, the phage library was created in such a manner as to allow wt-PrP to be represented at a very much higher level (six orders of magnitude higher) than that at which any of the other individual sequence variants was represented. While this difference existed in the input phage library used for the first biopanning step, it remained conceivable for phages possessing the ability to switch conformation and bind to β-PrP to overcome this lower representation if they possessed a tendency to bind to β-PrP that was several orders of magnitude higher than that of wt-PrP.

Our study enabled us to confirm that wt prion in the α-PrP conformation is capable of switching conformation to β-PrP and binding to the β-PrP presented on His-Sorb plates through simple bi-molecular interactions, at some basal level. What was especially satisfying was that this was achieved without the attendant complications usually accompanying unregulated aggregation and without our having to reckon for, and control, sizes of aggregates (note: this would have become necessary if $PrP^{Sc}$, instead of β-PrP, had been used for presentation, since it would be difficult to maintain uniformity of coating through successive rounds of biopanning with amyloid fibrillar aggregates).

Our use of such a library containing 25% wt-PrP-bearing phages helped us to identify variants capable of binding to β-PrP in the face of strong competition from wt prion. Both kinetic and thermodynamic considerations could be of importance, in this regard for a sequence variant could compete with wt prion either by (a) displaying a faster kinetics of switching to a β-PrP binding-competent conformation (because of its possessing a different sequence), or (b) through having already adopted a β-PrP binding-competent conformation, due to the sequence alterations, and through possession of a greater affinity for β-PrP than conformationally switched wt-PrP.

Our results with the recombinant MutPrP indicate the latter of the above scenarios to be likely to be the case. Most residues in the prion protein have a preference for β-conformation though the protein itself has a predominantly α-helical fold (Jackson et al., 1999b). Both variant prions obtained in this study show residue replacements with increased propensity for adoption of a β-sheet conformation (Table 3). The nature of residue replacements suggests that they could very well be much more prionogenic than wt prion, or at the very least more capable of binding to β-PrP through bimolecular reactions. The residue replacements also alter the hydrophobicity of the 101–112 region, and it is relevant to mention here that it has been suggested (Leffers et al., 2004) that the interactions of the N-terminal region with the rest of the prion polypeptide are largely hydrophobic.

Our study shows that the β-sheet-dominated conformation of wt PrP which can be created through refolding of the prion protein in acidic buffer (pH 4.0) under reducing conditions can also be naturally formed, under non-reducing conditions and at the alkaline pH of 10.0, by MutPrP which was selected through biopanning of a phage-displayed library of N-terminally randomized variants. The much greater propensity of this variant to form a β-sheet-rich structure, and to deposit into amyloid aggregates at near-neutral pH, appear to be completely in keeping with the fact that it was selected and amplified through four rounds of biopanning and amplification during screening for binding to β-PrP.

There is a β-sheet composed of two short strands in the structural core of the C-terminal domain of the prion protein. In the sequence, one of these strands is near the junction of the N- and C-terminal regions. The NMR structure of the human prion protein (Zahn et al., 2000) shows that both β-strands of the core β-sheet have interactions with the helices comprising the bulk of the C-terminal domain. It is possible that the

Table 3
Comparison of relative frequencies of occurrence of each of the amino acids to adopt a β-sheet conformation in the region between residues 101 and 112 of wt PrP, dominant variant (i) and the less observed variant (ii), as derived from Creighton (1983)

| Position | wt-PrP | Relative frequency | Variant (i) | Relative frequency | Variant (ii) | Relative frequency |
|---|---|---|---|---|---|---|
| 1 | K | 0.77 | K | 0.77 | V | 1.49 |
| 2 | P | 0.64 | G | 0.92 | R | 0.99 |
| 3 | S | 0.95 | V | 1.49 | L | 1.02 |
| 4 | K | 0.77 | L | 1.02 | L | 1.02 |
| 5 | P | 0.64 | T | 1.21 | D | 0.72 |
| 6 | K | 0.77 | W | 1.14 | L | 1.02 |
| 7 | T | 1.21 | F | 1.32 | T | 1.21 |
| 8 | N | 0.76 | S | 0.95 | S | 0.95 |
| 9 | M | 0.97 | P | 0.64 | G | 0.92 |
| 10 | K | 0.77 | L | 1.02 | V | 1.49 |
| 11 | H | 1.08 | W | 1.14 | S | 0.95 |
| 12 | M | 0.97 | Q | 0.8 | M | 0.97 |

increased hydrophobicity and β-sheet-forming propensity of the 101–112 region in MutPrP causes it to strip one of the core β-strands (the one near the C- and N-terminal junction in the sequence) away from its partner strand, and to hydrogen bond with it to form a β-sheet. This could cause the other strand, now free to try and form a β-sheet with any other part of the sequence, to pull away a region of the chain constituting a part of one of the surrounding helices away into a β-sheet-forming interaction. If this were to happen, this could start off a catastrophic process leading to the profound conformational transition that eventually occurs in the whole structure. Thus, we feel that our results – even as they reveal that identification of a super-amyloidogenic variant of the prion protein – highlight a possible mechanism by which mutations in the N-terminal region of the human prion protein ($PrP_{(90–231)}$) result in the conformational switching of the prion from a α-helical to a β-sheet-based structure.

## Acknowledgements

Dr. G. Sahni and Paramjit Kaur are thanked for assistance with N-terminal sequencing. Dr. V. Choudhary is thanked for the gift of the fdtetTA74 vector. Dr. Manoj Raje is thanked for assistance with the EM micrographs. Mr. Sanjeev Kumar, and Dr. B. Kundu are thanked for discussions at various stages.

## Appendix A. Supplementary data

Supplementary data associated with this article can be found, in the online version, at doi:10.1016/j.biocel.2007.10.009.

## References

Barron, R. M., Thomson, V., Jamieson, E., Melton, D. W., Ironside, J., Will, R., et al. (2001). Changing a single amino acid in the N-terminus of murine PrP alters TSE incubation time across three species barriers. *EMBO J.*, *20*, 5070–5078.

Collinge, J. (1997). Human prion disease and bovine spongiform encephalopathy (BSE). *Hum. Mol. Genet.*, *6*, 1699–1705.

Creighton, T. E. (1983). *Proteins: Structures and molecular properties*. NY: W.H. Freeman.

Goldfarb, L. G., Petersen, R. B., Tabaton, M., Brown, P., LeBlanc, A. C., Montagna, P., et al. (1992). Fatal familial insomnia and familial Creutzfeldt–Jacob disease: Disease phenotype determined by a DNA polymorphism. *Science*, *258*, 806–808.

Huang, Z., Gabriel, J. M., Baldwin, M. A., Fletterick, R. J., Prusiner, S. B., & Cohen, F. E. (1994). Proposed three-dimensional structure for the cellular prion protein. *Proc. Natl. Acad. Sci. U.S.A.*, *91*, 7139–7143.

Jackson, G. S., Hill, A. F., Joseph, C., Hosszu, L., Power, A., Waltho, J. P., et al. (1999a). Multiple folding pathways for heterogenously expressed human prion protein. *Biochem. Biophys. Acta*, *1431*, 1–13.

Jackson, G. S., Hill, A. F., Joseph, C., Hosszu, L., Power, A., Waltho, J. P., et al. (1999b). Reversible conversion of monomeric human prion protein between native and fibrillogenic conformation. *Science*, *283*, 1935–1937.

James, T. L., Liu, H., Ulyanov, N. B., Zhang, H., Donne, D. G., Kaneko, K., et al. (1997). Solution structure of a 142-residue recombinant prion protein corresponding to the infectious fragment of the scrapie isoform. *Proc. Natl. Acad. Sci. U.S.A.*, *16*, 10086–10091.

Leclerc, E., Peretz, D., Ball, H., Sakurai, H., Legname, G., Serban, A., et al. (2001). Immobilized prion protein undergoes spontaneous rearrangement to a conformation having features in common with the infectious form. *EMBO J.*, *20*, 1547–1554.

Leffers, K. W., Schell, J., Jansen, K., Lucassen, R., Kaimann, T., Nagel-Steger, L., et al. (2004). The structural transition of the prion protein into its pathogenic conformation is induced by unmasking hydrophobic sites. *J. Mol. Biol.*, *344*, 839–853.

Levy, Y., Hanan, E., Solomon, B., & Becker, O. M. (2001). Helix-coil transition of PrP 106–126: Molecular dynamic study. *Proteins*, *45*, 382–396.

Parmley, S. F., & Smith, G. P. (1988). Antibody-selectable filamentous fd phage vectors: Affinity purification of target genes. *Gene*, *73*, 305–318.

Peretz, D., Williamson, R. A., Matsunaga, Y., Serban, H., Pinilla, C., Bastidas, R. B., et al. (1997). A conformational transition at the N terminus of the prion protein features in formation of the scrapie isoform. *J. Mol. Biol.*, *273*, 614–622.

Prusiner, S. B., Bolton, D. C., Groth, D. F., Bowman, K. A., Cochran, S. P., & McKinley, M. P. (1982). Further purification and characterization of scrapie prions. *Biochemistry*, *21*, 6942–6950.

Prusiner, S. B., Scott, M. R., De Armond, S. J., & Cohen, F. E. (1998). Prion protein biology. *Cell*, *93*, 337–345.

Riek, R., Hornemann, S., Wider, G., Billeter, M., Glockshuber, R., & Wuthrich, K. (1996). NMR structure of the mouse prion protein domain PrP (121–231). *Nature*, *382*, 180–182.

Safar, J. G., Geschwind, M. D., Deering, C., Didorenko, S., Sattavat, M., Sanchez, H., et al. (2005). Diagnosis of human prion disease. *Proc. Natl. Acad. Sci. U.S.A.*, *102*, 3501–3506.

Sampath, A., Abrol, S., & Chaudhary, V. K. (1997). Versatile vectors for direct cloning and ligation-independent cloning of PCR amplified fragments for surface display on filamentous bacteriophage gene. *Gene*, *190*, 5–10.

Smith, G. P., & Scott, J. K. (1993). Libraries of peptides and proteins displayed on filamentous phage. *Methods Enzymol.*, *217*, 228–257.

Supattapone, S., Muramoto, T., Legname, G., Mehlhorn, I., Cohen, F. E., DeArmond, S. J., et al. (2001). Identification of two prion protein regions that modify scrapie incubation time. *J. Virol.*, *75*, 1408–1413.

Zahn, R., Liu, A., Luhrs, T., Riek, R., von Schroetter, C., Lopez Garcia, F., et al. (2000). NMR solution structure of the human prion protein. *Proc. Natl. Acad. Sci. U.S.A.*, *97*, 145–150.

Zhang, H., Kaneko, K., Nguyen, J. T., Livshits, T. L., Baldwin, M. A., Cohen, F. E., et al. (1995). Conformational transitions in peptides containing two putative alpha-helices of the prion protein. *J. Mol. Biol.*, *250*, 514–526.